40Ar/39Ar age constraints on the timing of magmatism and post-magmatic cooling in the Panagyurishte region, Bulgaria

Autor(en): **Handler, R. / Neubauer, F. / Velichkova, S.H.**

Objekttyp: **Article**

Zeitschrift: **Schweizerische mineralogische und petrographische Mitteilungen = Bulletin suisse de minéralogie et pétrographie**

Band (Jahr): **84 (2004)**

Heft 1-2: **Geodynamics and Ore Deposit Evolution of the Alpine-Carpathian-Balkan-Dinaride Orogenic System**

PDF erstellt am: **23.09.2024**

Persistenter Link: https://doi.org/10.5169/seals-63742

Schweizerische Mineralogische und Petrographische Mitteilungen 84, 119–132, 2004

$^{40}Ar/^{39}Ar$ age constraints on the timing of magmatism and post-magmatic cooling in the Panagyurishte region, Bulgaria

R. Handler[1], *F. Neubauer*[1], *S.H. Velichkova*[1,2] and *Z. Ivanov*[2]

Abstract

$^{40}Ar/^{39}Ar$ dating of amphibole and biotite from volcanic and plutonic rocks from the Panagyurishte region of the Srednogorie Zone (Bulgaria) shows a clear trend in post-magmatic cooling ages from north to south: A monzonite dyke from the Elatsite deposit yields ages of 90.78 ± 0.44 Ma (amphibole), and 91.72 ± 0.70 Ma (biotite). Further south, an andesite from the Vosdol neck exposed in the valley NE of Chelopech records an age of 89.95 ± 0.45 Ma (biotite). In the Medet mine, a coarse-grained granodiorite yields an age of 85.70 ± 0.35 Ma (amphibole), amphibole from a similar granodiorite from Elshitsa 84.07 ± 0.54 Ma. An andesite lava breccia exposed in the Sv. Nikola hill south of Panagyurishte records an age of 80.21 ± 0.45 Ma (amphibole). Our new $^{40}Ar/^{39}Ar$ ages are in line with recently reported U–Pb zircon ages. Older subvolcanic rocks (ca. 92–90 Ma) developed in a regime of ca. N–S extension. They show that the southward prograding magmatism is older than dextral shear, which developed between ca. 86–78 Ma within a ca. N–S compressional tectonic regime.

Keywords: Collapse basin, arc magmatism, extension, Cretaceous, back arc basin, mineralization, $^{40}Ar/^{39}Ar$ geochronology.

Introduction

The nature and evolution of the so-called Banatite Belt of southeastern Europe (von Cotta, 1864), a belt of Late Cretaceous volcanic, subvolcanic, and shallow plutonic rocks with widespread mineralizations, are still enigmatic. The Banatite Belt extends from the Black Sea through the Bulgarian Srednogorie Zone and the Serbian Timok-Majdanpek area to the Romanian Apuseni Mountains, and possibly to the Western Carpathians (Fig. 1; e.g., Jankovic, 1997; Berza et al., 1998; Ciobanu et al., 2002). Although much work has been done because of its high economic importance with numerous Cu–Au epithermal and other mineralizations, the tectonic evolution of the Banatite Belt is not fully understood (e.g., Berza et al., 1998; Ciobanu et al., 2002; Neubauer, 2002; von Quadt et al., 2002). Several models of geodynamic setting were proposed for the formation of the Banatite Belt including the Srednogorie Zone: (1) rift (Popov, 1987), (2) subduction (Berza et al., 1998) and (3) possible post-collisional slab break-off (Neubauer, 2002). The arguments mainly came from geochemistry of magmatic rocks with its predominance of calcalkaline rocks supporting the idea of subduction (e.g. Boccaletti et al., 1974; von Quadt et al., 2002), relationships to slightly older ductile deformation and metamorphism (Ciobanu et al., 2002; Neubauer, 2002; Velichkova et al., 2004) and type of basin formation (Aiello et al., 1977).

Here we present new $^{40}Ar/^{39}Ar$ ages of magmatic minerals from the Pangyurishte region, where a NNW trend of Banatite magmatism formed across the principal E–W striking Srednogorie Zone. This trend seems to be particularly important because of its richness of magmatic rocks and associated ore deposits (Strashimirov and Popov, 2000).

In conjunction with recent U–Pb zircon ages from other authors (e.g. von Quadt et al., 2002; Table 1) the new data may help to elucidate aspects of the tectonic evolution of the particularly important Panagyurishte region in Bulgaria, especially the duration of magmatism and some effects of possible thermal overprint. Finally, based on some structural data and interpretation of previously reported structures, we speculate on models of the Late Cretaceous tectonic evolution of the Panagyurishte region.

[1] Institute of Geology and Palaeontology, University of Salzburg, Hellbrunner Str. 34, A-5020 Salzburg, Austria. <robert.handler@ sbg.ac.at>
[2] Dept. of Geology, Sofia University, Sofia, Tzar Osvoboditel Blv. 15, Sofia 1000, Bulgaria.

0036-7699/04/0084/119

Fig. 1 Overview map of southeastern Europe displaying the U-shaped Banatite-Srednogorie Zone. P—Panagyurishte corridor.

Geological setting

The principal Cretaceous structures of the Alpine-Balkan-Carpathian-Dinaride (ABCD) orogen are that of a thick-skinned orogenic wedge, which formed in response to collision of continental microplates (Channell and Kozur, 1997; Ricou et al., 1998; Neubauer, 2002). The principal Late Jurassic to Cretaceous orogenic structures are common features for the whole internal Cretaceous ABCD belt. As it is now well established, we can distinguish between (1) Late Jurassic obduction of oceanic crust in Dinaric, Vardar, Mures and Meliata ophiolite belts, (2) Early Cretaceous to early Late Cretaceous collisional structures, mainly ductile thrusts, and (3) Late Cretaceous formation of collapse sedimentary basins, which are in southeastern sectors associated with Banatite magmatism, and associated ductile low-angle normal and high-angle strike-slip faults, which relate to basin formation (Neubauer et al., 1995; Ricou et al., 1998; Willingshofer et al., 1999).

The Bulgarian Balkan region is linked through the Serbian Timok zone with the extension of the Southern Carpathians surrounding the western Moesian platform. In Bulgaria, the zone with specific Late Cretaceous sedimentary/volcanogenic basins is called Srednogorie Zone (Fig. 1; Aiello et al. 1977; Bocaletti et al. 1974, 1978; Popov, 1987; Popov and Popov, 2000; Ciobanu et al., 2002). The Srednogorie Zone extends to the Black Sea, where it is superposed onto the southerly adjacent Strandja zone (with mainly Late Jurassic tectonism; Okay et al., 2001; S of Burgas in Fig. 1). The central Srednogorie Zone (Fig. 2) comprises a pre-Alpine basement (e.g., Dabovski, 1988; Arnaudov et al., 1989), a late Carboniferous to Triassic cover succession, and, above a pronounced angular unconformity, the Senonian Srednogorie Group (e.g., Karagjuleva et al., 1974; Aiello et al., 1977; Foose and Manheim, 1975; Ivanov et al., 2002). The basement of the Srednogorie Zone experienced an amphibolite-grade late Variscan and low-grade early Late Cretaceous metamorphism and associated ductile deformation between 105 and 99 Ma (Velichkova et al., 2001, 2004). Metamorphic overprint also affected the Late Palaeozoic-Triassic cover and increases from very low-grade conditions in the north to low-grade (greenschist facies) conditions in the south. There, metamorphic overprint was associated with ductile top-W shear (Ivanov et al., 2002).

After a short period of erosion and denudation, the Srednogorie volcano-sedimentary basin was formed, with the Srednogorie Group representing the basin infill. The stratigraphic range of the Srednogorie Group is from Coniacian to Maastrichtian (Ivanov et al., 2002; Aiello et al., 1977). The basin fill mainly comprises clastic terrigeneous sequences with subordinate pelagic marls, shales, turbidites, and three levels of volcanic intercalations (Aiello et al., 1977; Ivanov et al., 2002). Because of the calcalkaline magmatism, the Srednogorie Zone is interpreted to represent an intra-arc basin (e.g., Aiello et al., 1977) or post-collisional successor- or rift-type basin (e.g., Popov, 1987; Popov and Popov, 2000).

Late Cretaceous high-level plutonic suites, collectively referred to as "Banatites", and some subordinate volcanic sequences (von Cotta, 1864) extend from the northern Apuseni Mountains in Romania to the Black Sea (Fig. 1). Many different terms have been proposed for this belt, e. g. Apuseni-Banat-Timok-Srednogorie Magmatic and Metallogenetic Belt (Berza et al., 1998 and references therein), but for simplicity we here use the term "Banatite Belt". These Banatites are associated with various types of mineralization including porphyry copper, epithermal and replacement ores (Popov, 1987, 1996; Berza et al. 1998; Popov and Popov, 2000; Ciobanu et al., 2002; Tarkian et al., 2003). Calcalkaline suites largely predominate, although minor alkaline rocks were reported from the Bulgarian Srednogorie Zone (e.g., Bocalletti et al. 1974, 1978; Berza et al., 1998 and references therein). In the Panagyurishte region, a specific NNW trend across the generally E–W striking Srednogorie Zone hosts numerous, predominantly shallow intrusive bodies (Srednogorie-type intrusions according to Ivanov et al., 2002; Fig. 2) with associated Cu–Au epithermal, porphyry and massive sulphide mineralizations (Strashimirov and Popov, 2000; Kouzmanov et al., 2003; Tarkian et al., 2003). Srednogorie-type intrusions were distinguished from Rhodope-type intrusions according to their country rocks (Ivanov, unpubl. data).

Recent U–Pb zircon age data from Banatite volcanic and plutonic rocks exposed in the Panagyurishte region are compiled in Table 1. Peytcheva et al. (2001), von Quadt et al. (2002, 2003a), Stoykov et al. (2004), and Peytcheva and von Quadt et al. (2003) reported U–Pb zircon ages ranging between 92.3 and 78.6 Ma (Table 1) from several plutons.

The Alpine metamorphic overprint predated Banatite magmatism, reached low-grade conditions and is dated at 105 to 99 Ma by the $^{40}Ar/^{39}Ar$ method (Velichkova et al., 2001, 2004). Afterwards, a number of post-collisional basins formed, which are associated with calc-alkaline and subordinate alkaline volcanic and some subvolcanic and plutonic rocks, which are partly rich in ore mineralizations (Aiello et al., 1977; Berza et al., 1998; Boccaletti et al., 1974, 1978).

The WNW-striking steep brittle Cenozoic Maritsa fault is superimposed on the Late Cretaceous Iskar-Yavoritsa ductile shear zone in south-

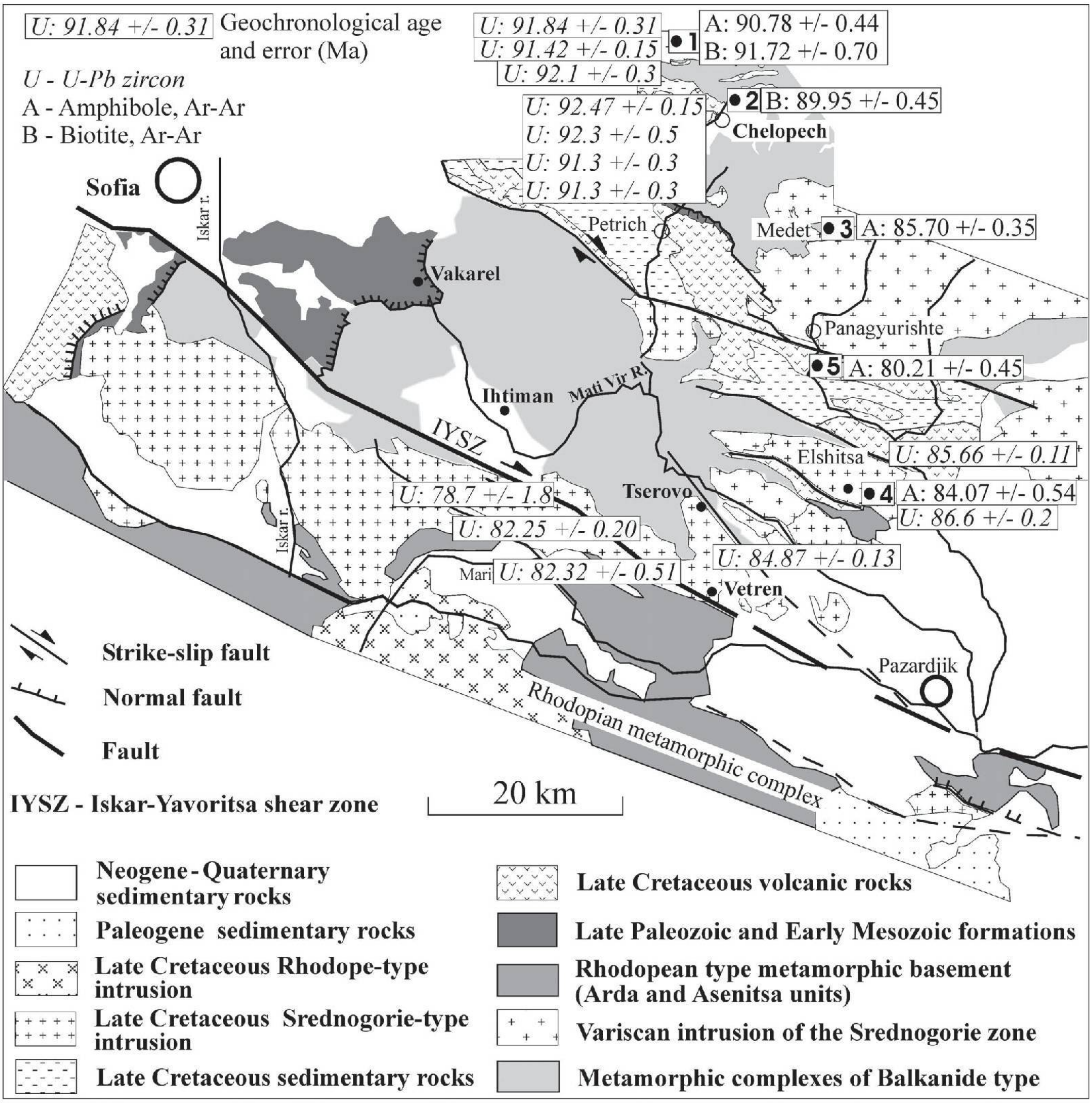

Fig. 2 Simplified tectonic map of the Panagyurishte corridor in the Srednogorie Zone and the northern margin of the Rhodope massif displaying sample locations (bold numbers).

Table 1 Compilation of U–Pb ages from the Srednogorie Zone.

Locality	Rock type	Age and error (Ma)	Reference
Elatsite	quartz monzonite porphyry	92.1 ± 0.3	von Quadt et al. (2002)
Elatsite	diorite porphyry	91.84 ± 0.31	von Quadt et al. (2002)
Elatsite	granodiorite porpyhry	91.42 ± 0.15	von Quadt et al. (2002)
Chelopech	andesite	91.47 ± 0.15	Chambefort et al. (2003)
Chelopech	andesite I phase	92.3 ± 0. 5	Stoykov et al. (2004)
Chelopech	trachydacite II phase	91.3 ± 0.3	Stoykov et al. (2004)
Chelopech	andesite III phase	91.3 ± 0.3	Stoykov et al. (2004)
Elshitsa	granite	86.6 ± 0.1	Peytcheva et al. (2003)
Elshitsa	subvolc. dacite	86.1 ± 0.2	Peytcheva et al. (2003)
Vlaikov vrach	hydrothermal rutile	85.66 ± 0.11	Peytcheva et al. (2003)
Velichkovo	granodiorite	84.6 ± 0.3	Peytcheva and von Quadt (2003)
Velichkovo	gabbro	82.16 ± 0.10	Peytcheva and von Quadt (2003)
Vetren	hybrid gabbro	84.87 ± 0.13	Peytcheva and von Quadt (2003)
Vershilo	granite	82.25 ± 0.20	Peytcheva et al. (2001)
Capitan Dimitrievo	monzodiorite (hybrid gabbro)	78.6 ± 0.3	Kamenov et al. (2002)

ern sectors of the Panagyurishte region (Fig. 2) and separates the Srednogorie Zone from the southerly adjacent Rhodope massif. The Iskar-Yavoritsa fault also includes sheared Late Cretaceous granites intruded between 84 and 78 Ma (Kamenov et al., 2002; von Quadt et al., 2002, 2003b). In the Rhodope massif, the uppermost unit is a Cretaceous metamorphic unit, which formed within Cretaceous amphibolite facies metamorphic conditions (e.g., Burg et al., 1990, 1993; Ricou et al., 1998; Krohe and Mposkos, 2002). Furthermore, the data suggest that the Iskar-Yavoritsa shear zone and its splays to the N (e.g., Kamenitsa-Rakovitsa fault zone) can together be regarded as a Cretaceous dextral wrench corridor, which was active under greenschist facies metamorphic conditions. The zone is intruded by Late Cretaceous granites and diorites, which are partly affected by ductile shearing. The age of intrusions varies between 84 and 78 Ma (von Quadt et al., 2002), which therefore represent the minimum duration of dextral shearing as only plutons of this age interval have been affected. Subsidence of the Srednogorie basin is contemporaneous with exhumation and surface uplift in the Rhodopes (e.g. Ricou et al., 1998). The Rhodopian metamorphic complex extends from Bulgaria to Greece and westernmost Turkey, and comprises a stack of metamorphic nappes (Ricou et al., 1998; Krohe and Mposkos, 2002, and references therein), which are younging in age of metamorphism towards the footwall. This matches the interpretation of a southerly located hinterland of clastic successions in the Srednogorie basin (Aiello et al., 1977), which can be identified as the Rhodope massif (respectively Rhodopian metamorphic complex: Fig. 2).

$^{40}Ar/^{39}Ar$ analytical techniques

Preparation of the samples before and after irradiation, $^{40}Ar/^{39}Ar$ analyses, and age calculations were carried out at the ARGONAUT Laboratory of the Institute for Geology and Palaeontology at the University Salzburg. Mineral concentrates are packed in aluminium-foil and loaded in quartz vials. For calculation of the J-values, flux-monitors are placed between each 4–5 unknown samples, which yield a distance of ca. 5 mm between adjacent flux-monitors. The sealed quartz vials are irradiated in the MTA KFKI reactor (Debrecen, Hungary) for 16 hours. Correction factors for interfering isotopes were calculated from 10 analyses of two Ca-glass samples and 22 analyses of two pure K-glass samples, and are: $^{36}Ar/^{37}Ar_{(Ca)}$ = 0.00026025, $^{39}Ar/^{37}Ar_{(Ca)}$ = 0.00065014, and $^{40}Ar/^{39}Ar_{(K)}$ = 0.015466. Variation in the flux of neutrons were monitored with DRA1 sanidine standard for which a $^{40}Ar/^{39}Ar$ plateau age of 25.03 ± 0.05 Ma has been reported (Wijbrans et al., 1995). After irradiation the minerals are unpacked from the quartz vials and the aluminium-foil packets, and hand-picked into 1 mm diameter holes of the one-way Al-sample holders.

$^{40}Ar/^{39}Ar$ analyses are carried out using a UHV Ar-extraction line equipped with a combined MERCHANTEK™ UV/IR laser system, and a VG-ISOTECH™ NG3600 mass spectrometer.

Stepwise heating analyses of samples are performed using a defocused (~1.5 mm diameter) 25 W CO_2-IR laser operating in Tem_{00} mode at wavelengths between 10.57 and 10.63 μm. The laser is controlled from a PC, and the position of the laser on the sample is monitored on the computer screen via a video camera in the optical axis of the laser beam through a double-vacuum window on the sample chamber. Gas clean-up is performed using one hot and one cold Zr–Al SAES getter. Gas admittance and pumping of the mass spectrometer and the Ar-extraction line are computer controlled using pneumatic valves. The NG3600 is a 18 cm radius 60° extended geometry instrument, equiped with a bright Nier-type source operated at 4.5 kV. Measurements are performed on an axial electron multiplier in static mode, peak-jumping and stability of the magnet is controlled by a Hall-probe. For each increment the intensities of ^{36}Ar, ^{37}Ar, ^{38}Ar, ^{39}Ar, and ^{40}Ar are measured, the baseline readings on mass 35.5 are automatically subtracted. Intensities of the peaks are back-extrapolated over 16 measured intensities to the time of gas admittance either by a straight line or a curved fit, depending on intensity and type of pattern of the evolving gas. Intensities are corrected for system blanks, background, post-irradiation decay of ^{37}Ar, and interfering isotopes. Isotopic ratios, ages and errors for individual steps are calculated following suggestions by McDougall and Harrison (1999) using decay factors reported by Steiger and Jäger (1977). Definition and calculation of plateau ages has been carried out using ISOPLOT/EX (Ludwig, 2001).

$^{40}Ar/^{39}Ar$ dating results

$^{40}Ar/^{39}Ar$ amphibole and biotite concentrates of volcanic, subvolcanic, and plutonic rocks from five locations (Fig. 2) were studied. Only well-preserved biotite and amphibole grains without visible signs of secondary alteration were selected for dating. This sampling strategy should avoid bias in the age interpretation that may arise from post-magmatic alteration including hydrothermal alteration related to mineralizing fluids as these reached relatively high temperatures (ca. 300–400 °C; e. g. Strashimirov et al., 2002; Kehayov et al., 2003; Tarkian et al., 2003), which are above the argon retention temperature of biotite. The dated samples are described in the Appendix. $^{40}Ar/^{39}Ar$ dating results are presented in Table 2 and graphically shown in Fig. 3. A few biotite grains in thin sections from these samples display, however, some variable but minor and clearly recognizable hydrothermal alteration suggesting a weak post-magmatic thermal overprint. Some biotite concentrates show low-temperature overprint in low-energy steps of the experiment.

Sample 1 is a largely unaltered quartz monzonite dyke from the Elatsite deposit (as also dated by von Quadt et al., 2002), which yielded a perfect plateau (steps 1–8: 99.9% ^{39}Ar released) recording an age of 90.78 ± 0.44 Ma for the amphibole (sample 1a). The Ar-release pattern of the biotite (sample 1b) shows major fluctuations in the low-temperature gas release steps (first 12.6% of the total ^{39}Ar released). Ages reported for the first three steps (5.6% ^{39}Ar released) range between ca. 32 and 110 Ma, then (steps 4–6: 6.0% ^{39}Ar released) the Ar-release plot reveals a staircase type pattern with increasing ages from ca. 34 to 73 Ma, and finally reaches a plateau age (steps 7–16: 87.4% ^{39}Ar released) of 91.72 ± 0.70 Ma. This disturbed age pattern indicates that, in contrast to amphibole, the biotite has significantly been thermally altered by a subsequent event with a maximum age of ca. 32 Ma. This alteration probably also allowed incorporation of minor excess ^{40}Ar-components. Therefore, the completely flat age-spectrum of the amphibole (sample 1a) is regarded to be more significant. However, both $^{40}Ar/^{39}Ar$ ages are similar within the range of the 1 σ error, and are slightly younger than recently reported U–Pb zircon ages of 92.1 ± 0.3 Ma and 91.84 ± 0.3 Ma (von Quadt et al., 2002) obtained from the same rock type at this locality.

Biotite was separated from a coarse-grained, brecciated andesite block (sample 2), enclosed in a fine-grained andesite matrix from the Vosdol neck exposed in the valley NE of Chelopech (Strashimirov and Popov, 2000). The first step records an age of ca. 40 Ma (Eocene), while the rest of the Ar-release plot indicates a nearly flat pattern resulting in a plateau age (steps 2–13: 86.0% ^{39}Ar released) of 89.95 ± 0.45 Ma. Again, this age is similar, though slightly younger, than a U–Pb zircon age of 91.45 ± 0.15 Ma reported for a nearby located, altered and mineralized andesite of Chelopech (Chambefort et al., 2003).

An amphibole concentrate from a porphyric granodiorite (sample 3) of the Medet open pit yielded a perfectly flat plateau age of 85.70 ± 0.35 Ma (steps 1–11: 100% ^{39}Ar released).

From the Elshitsa open pit an amphibole concentrate from a granodiorite (sample 4) yielded a slightly disturbed age pattern with minor fluctuations in the first six release steps. The first three steps (together comprising 2.1% ^{39}Ar released) have ages between ca. 120 and 40 Ma, which indicate excess ^{40}Ar components incorporated in a least retentive, optically not resolvable, mineralogical phase. Then, the Ar-release plot indicates a staircase-type pattern with inc reasing ages from ca. 39 Ma (Eocene) to ca. 73 Ma, and finally defines a plateau (steps 7–14: 93.3% ^{39}Ar released) with an age of 84.07 ± 0.54 Ma.

An amphibole concentrate was obtained from a porphyric andesite lava breccia (sample 5) exposed in the Sv. Nikola hill south of Panag-

Table 2 Ar-analytical data from laser-step-heating experiments on amphibole and biotite multi-grain samples from Banatites of the Panagyuriste ore region, Bulgaria.

Sample 1a Elatsite Amphibole (160–224 μm)
J-Value: 0.02228 +/- 0.00022

step	$^{36}Ar/^{39}Ar^a$	+/-	$^{37}Ar/^{39}Ar^b$	+/-	$^{40}Ar/^{39}Ar^a$	+/-	$\%^{40}Ar^c$	$\%^{39}Ar$	age [Ma]	+/-
1	0.00865	0.00016	2.73891	0.00017	4.754	0.049	46.3	3.1	93.94	2.07
2	0.00126	0.00002	2.99531	0.00003	2.472	0.005	85.0	22.6	90.92	0.91
3	0.00148	0.00019	3.32727	0.00022	2.568	0.056	83.0	1.6	93.11	2.33
4	0.00106	0.00003	3.02434	0.00004	2.411	0.009	87.0	13.4	90.94	0.95
5	0.00108	0.00001	2.87325	0.00002	2.399	0.004	86.7	33.6	89.72	0.89
6	0.00107	0.00002	3.04538	0.00002	2.397	0.006	86.9	25.2	90.37	0.91
7	0.00172	0.00079	7.78932	0.00105	2.834	0.233	82.1	0.3	113.92	8.85
8	0.00527	0.00242	11.99402	0.00285	3.225	0.715	51.7	0.1	101.42	27.18
9	0.00546	0.00253	21.98991	0.00336	3.141	0.749	48.6	0.1	126.11	28.10
steps 1-8 =plateau age:								99.9	90.78	0.44

Sample 1b Elatsite Biotite (160–224 μm)
J-Value: 0.02227 +/- 0.00022

step	$^{36}Ar/^{39}Ar^a$	+/-	$^{37}Ar/^{39}Ar^b$	+/-	$^{40}Ar/^{39}Ar^a$	+/-	$\%^{40}Ar^c$	$\%^{39}Ar$	age [Ma]	+/-
1	0.08810	0.00157	0.06465	0.00136	26.859	0.471	3.1	1.0	32.49	18.60
2	0.02021	0.00070	0.01220	0.00068	7.136	0.208	16.3	2.2	45.55	8.14
3	0.00431	0.00041	0.00234	0.00041	4.121	0.120	69.1	3.4	110.30	4.67
4	0.00957	0.00149	0.01678	0.00155	3.698	0.441	23.5	0.9	34.02	17.40
5	0.00647	0.00054	0.01901	0.00055	3.813	0.160	49.9	2.5	74.29	6.20
6	0.00348	0.00049	0.00328	0.00062	2.907	0.145	64.7	2.6	73.38	5.65
7	0.00194	0.00020	0.01688	0.00016	2.899	0.060	80.2	7.8	90.58	2.44
8	0.00202	0.00016	0.01824	0.00012	2.993	0.047	80.1	11.0	93.27	2.00
9	0.00901	0.00018	0.01882	0.00012	5.097	0.052	47.8	9.7	94.72	2.19
10	0.00083	0.00020	0.01976	0.00016	2.626	0.060	90.6	7.2	92.62	2.45
11	0.00025	0.00008	0.02279	0.00007	2.424	0.023	97.0	19.9	91.53	1.25
12	0.00017	0.00021	0.00715	0.00018	2.399	0.063	97.9	7.7	91.42	2.55
13	0.00019	0.00013	0.00342	0.00010	2.353	0.038	97.6	12.8	89.39	1.70
14	0.00003	0.00035	0.00714	0.00026	2.384	0.103	99.6	4.7	92.36	4.04
15	0.00014	0.00036	0.00529	0.00026	2.376	0.107	98.3	4.8	90.88	4.19
16	0.00046	0.00085	0.01351	0.00073	2.498	0.250	94.6	1.9	91.93	9.58
steps 7-16 =plateau age:								87.4	91.72	0.70

Sample 2 Chelopech Biotite (160–224 μm)
J-Value: 0.02230 +/- 0.00022

step	$^{36}Ar/^{39}Ar^a$	+/-	$^{37}Ar/^{39}Ar^b$	+/-	$^{40}Ar/^{39}Ar^a$	+/-	$\%^{40}Ar^c$	$\%^{39}Ar$	age [Ma]	+/-
1	0.01051	0.00071	0.02153	0.00074	4.118	0.210	24.6	1.2	39.73	8.29
2	0.00337	0.00059	0.01018	0.00071	3.091	0.174	67.7	1.3	81.75	6.73
3	0.00171	0.00032	0.00190	0.00037	2.671	0.095	81.0	2.7	84.47	3.73
4	0.00096	0.00010	0.00403	0.00013	2.583	0.028	89.0	7.1	89.61	1.39
5	0.00034	0.00015	0.00198	0.00017	2.515	0.045	96.0	5.0	93.99	1.94
6	0.00014	0.00012	0.00179	0.00011	2.411	0.036	98.3	7.6	92.30	1.64
7	0.00015	0.00008	0.00179	0.00006	2.340	0.024	98.2	11.7	91.78	1.28
8	0.00024	0.00013	0.00015	0.00010	2.428	0.039	97.1	7.5	91.85	1.75
9	0.00008	0.00013	0.00068	0.00011	2.343	0.038	99.0	7.6	90.38	1.70
10	0.00038	0.00005	0.00593	0.00007	2.388	0.016	95.2	11.1	88.69	1.06
11	0.00028	0.00006	0.00057	0.00008	2.342	0.019	96.5	11.9	88.14	1.13
12	0.00032	0.00009	0.00153	0.00012	2.380	0.027	96.1	7.9	89.12	1.34
13	0.00027	0.00016	0.00328	0.00020	2.380	0.047	96.6	4.7	89.63	1.99
14	0.00052	0.00015	0.00096	0.00017	2.385	0.043	93.6	5.3	87.04	1.87
15	0.00023	0.00013	0.00043	0.00014	2.263	0.038	96.9	6.4	85.55	1.66
16	0.00130	0.00072	0.01031	0.00091	2.392	0.212	83.9	1.0	78.45	8.21
steps 2-13 =plateau age:								86.0	89.95	0.45

Table 2 (continued)

Sample 3 Medet Amphibole (160–224 µm)
J-Value: 0.02229 +/- 0.00022

step	$^{36}Ar/^{39}Ar^a$	+/-	$^{37}Ar/^{39}Ar^b$	+/-	$^{40}Ar/^{39}Ar^a$	+/-	$\%^{40}Ar^c$	$\%^{39}Ar$	age [Ma]	+/-
1	0.03406	0.00031	5.61957	0.00022	11.956	0.094	15.8	3.5	90.82	3.71
2	0.00322	0.00006	5.14379	0.00006	2.802	0.016	66.1	12.4	87.87	1.06
3	0.00223	0.00004	5.12337	0.00004	2.463	0.011	73.2	20.5	85.94	0.94
4	0.00248	0.00007	5.75886	0.00009	2.447	0.019	70.0	7.4	84.42	1.11
5	0.00214	0.00004	5.18404	0.00003	2.446	0.012	74.2	15.2	86.56	0.97
6	0.00268	0.00005	5.78344	0.00006	2.540	0.016	68.8	8.3	85.80	1.04
7	0.00316	0.00005	6.52397	0.00010	2.566	0.014	63.6	9.4	83.67	0.98
8	0.00234	0.00006	5.07759	0.00007	2.461	0.017	71.9	9.0	84.51	1.05
9	0.00236	0.00005	4.94356	0.00007	2.538	0.015	72.6	10.7	86.90	1.01
10	0.00270	0.00011	5.72343	0.00019	2.517	0.031	68.4	3.1	84.59	1.46
11	0.00635	0.00093	13.48377	0.00116	2.868	0.275	34.6	0.4	79.87	10.62
steps 1-11 =plateau age:								100.0	85.70	0.35

Sample 4 Elshitsa Amphibole (250–355 µm)
J-Value: 0.02211 +/- 0.00022

step	$^{36}Ar/^{39}Ar^a$	+/-	$^{37}Ar/^{39}Ar^b$	+/-	$^{40}Ar/^{39}Ar^a$	+/-	$\%^{40}Ar^c$	$\%^{39}Ar$	age [Ma]	+/-
1	0.21757	0.00131	2.16948	0.00149	67.357	0.413	4.5	1.0	124.08	15.44
2	0.11130	0.00208	1.76162	0.00237	33.681	0.628	2.3	0.5	36.01	24.54
3	0.07130	0.00176	1.96938	0.00189	24.082	0.525	12.5	0.6	121.61	19.60
4	0.04861	0.00065	7.65782	0.00144	14.762	0.195	2.7	1.6	38.57	7.62
5	0.02841	0.00075	16.24681	0.00308	8.508	0.223	1.3	1.0	53.48	8.64
6	0.02040	0.00048	10.66579	0.00136	7.077	0.143	14.8	1.9	72.92	5.50
7	0.02104	0.00020	12.96929	0.00070	7.347	0.058	15.4	5.6	83.02	2.35
8	0.01172	0.00006	12.48276	0.00020	4.674	0.018	25.9	25.1	84.64	1.07
9	0.00610	0.00007	11.88285	0.00023	3.014	0.020	40.2	24.8	82.91	1.11
10	0.00527	0.00006	12.09969	0.00028	2.755	0.017	43.5	17.0	82.98	1.05
11	0.00678	0.00009	12.72930	0.00034	3.266	0.026	38.7	14.0	87.39	1.30
12	0.00729	0.00044	11.27083	0.00127	3.300	0.131	34.7	2.3	78.52	5.07
13	0.00695	0.00054	11.54070	0.00181	3.277	0.158	37.3	2.2	82.30	6.09
14	0.00679	0.00047	11.03383	0.00130	3.281	0.138	38.8	2.3	82.73	5.31
steps 7-14 =plateau age:								93.3	84.07	0.54

Sample 5 Sv. Nicola Amphibole (160–224 µm)
J-Value: 0.02226 +/- 0.00022

step	$^{36}Ar/^{39}Ar^a$	+/-	$^{37}Ar/^{39}Ar^b$	+/-	$^{40}Ar/^{39}Ar^a$	+/-	$\%^{40}Ar^c$	$\%^{39}Ar$	age [Ma]	+/-
1	0.05656	0.00047	0.96309	0.00037	21.411	0.140	21.9	2.4	181.60	5.38
2	0.02688	0.00113	2.11392	0.00094	9.379	0.334	15.3	0.9	62.55	12.95
3	0.02156	0.00085	1.93196	0.00086	7.314	0.251	12.9	1.0	42.83	9.84
4	0.01796	0.00076	1.64342	0.00066	7.186	0.224	26.1	1.3	78.24	8.65
5	0.00934	0.00084	2.09383	0.00094	5.375	0.248	48.6	1.0	107.72	9.45
6	0.01895	0.00082	2.51845	0.00076	6.603	0.242	15.2	1.0	46.91	9.46
7	0.01111	0.00034	4.55652	0.00048	4.211	0.100	22.0	2.2	50.13	3.91
8	0.00381	0.00008	7.09746	0.00011	2.670	0.024	57.9	11.6	81.85	1.21
9	0.00423	0.00008	6.39483	0.00017	2.735	0.024	54.3	10.7	77.36	1.18
10	0.00428	0.00006	6.74497	0.00012	2.813	0.019	55.0	14.8	80.86	1.08
11	0.00367	0.00007	6.69726	0.00010	2.624	0.021	58.7	14.2	80.49	1.12
12	0.00454	0.00007	7.46503	0.00016	2.788	0.022	51.9	7.5	79.16	1.13
13	0.00337	0.00004	7.35856	0.00005	2.500	0.013	60.2	30.8	81.07	0.93
14	0.00667	0.00122	8.31726	0.00162	3.198	0.360	38.4	0.6	73.28	13.91
steps 8-14 =plateau age:								90.2	80.21	0.45

Errors of ratios, J-values, and ages are at 1-sigma level.
[a] measured
[b] corrected for post-irradiation decay of ^{37}Ar
[c] non atmospheric ^{40}Ar

yurishte, which shows no mineralization (stop 5 of Excursion A in Strashimirov and Popov, 2000). Similar to sample 4, this sample records a slightly disturbed age spectrum, indicating incorporation of excess ^{40}Ar components in a least retentive phase (steps 1–5: 6.6% ^{39}Ar released). Again, the next steps indicate a staircase-type pattern with increasing ages from ca. 47 Ma (Eocene) to ca. 77 Ma, and finally defines a plateau (steps 8–14: 90.2% ^{39}Ar released) recording an age of 80.21 ± 0.45 Ma.

Discussion

Significance of $^{40}Ar/^{39}Ar$ ages

Our new $^{40}Ar/^{39}Ar$ ages from magmatic rocks of the Panagyurishte ore region are basically in line with recent U–Pb zircon ages (von Quadt et al. 2002, 2003a; Chambefort et al., 2003; Kamenov et al., 2002; for full references and data set, see Table 1). Ages of samples 1, 2 and 5 record rapid cooling

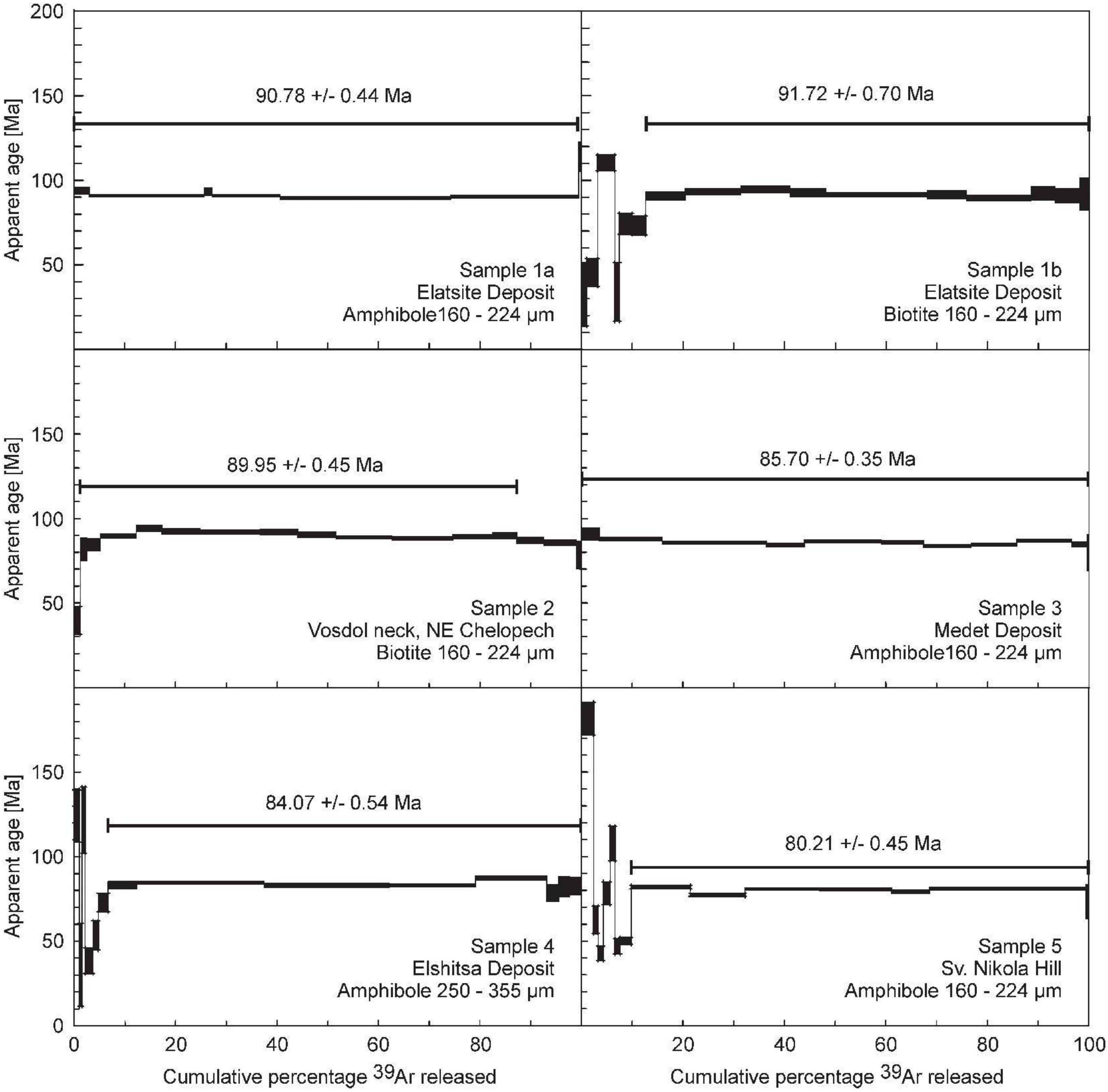

Fig. 3 $^{40}Ar/^{39}Ar$ apparent age spectra of amphibole and biotite multi-grain samples (ca. 10–20 grains for each sample) from volcanic and subvolcanic rocks of the Banatite Belt exposed in the Panagyurishte corridor. Laser energy increases from left to right. Vertical width of bars represents 1σ errors. Steps used for calculation of plateau ages are delineated by bar.

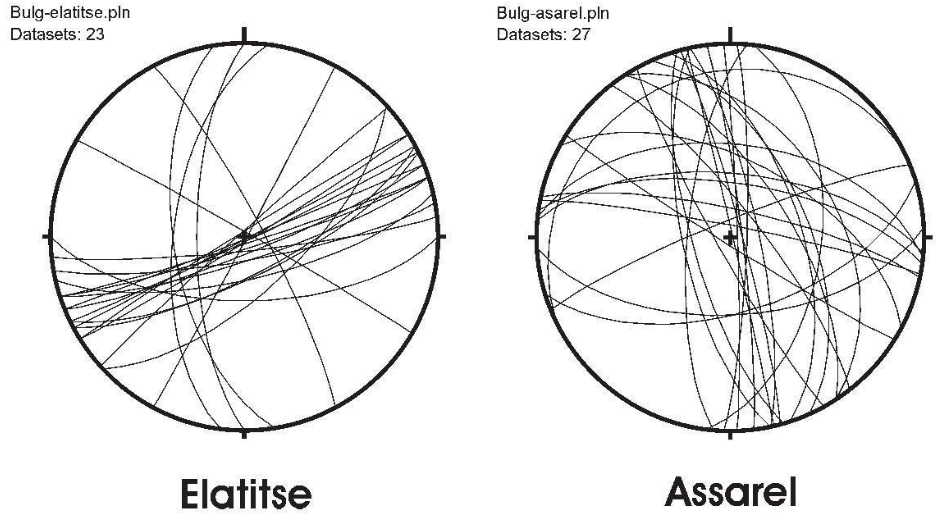

Fig. 4 Orientation data of mineralized extension veins from several mineralizations. These indicate ca. N–S to SSE–NNW extension (Elatsite) and predominant E–W extension for Assarel.

after magma emplacement as dated rocks are of subvolcanic and volcanic origin. The biotite age (89.98 ± 0.45) of the Vosdol neck andesite is ca. 1.3 Ma younger than U–Pb zircon ages from a variety of other andesite types from the Chelopech area (see Table 1). As no alteration of biotite was detected, the age is interpreted to date a younger stage of volcanism in the Chelopech region.

In contrast, the ages from samples 3 and 4 are shallow-level plutonic rocks and record the age of cooling, which seems to be, in the case of Elshitsa, ca. 2 Ma younger than the age of magma emplacement as recorded by the U–Pb zircon ages (86.6 ± 0.1 Ma for granite and 86.1 ± 0.2 Ma for subvolcanic dacite; but note that our dated rock from Elshitsa are is not from the same type as those of Peytcheva et al., 2003). Because of some alteration of amphibole grains from the dated granodiorite sample of Elshitsa, we cannot exclude the possibility of having dated alteration at 84.07 ± 0.54 Ma. This alternative interpretation would explain the ca. 2 Ma age difference compared with the U–Pb zircon age, but this needs further confirmation.

Magmatism within the Panagyurishte area was likely not continuous as indicated by three major volcanic levels exposed in the southern Central Srednogorie basin. These include a group with ages between 92 and 89 Ma in the northernmost area, then an age group at ca. 85–84 Ma in mid of the N–S trending Panagyurishte corridor, and a final age group between 84 and 78, basically in the south (except our sample 5). The latter group of magmatic rocks seems to be barren. An alternative interpretation would be, that the absence of mineralization may reflect a deeper erosional level. In a large scale, the new age data suggest a north-to-south age progression, except for the not mineralized andesite of Sv. Nikola hill, which yielded an age of ca. 84 Ma. This trend seems similar to an E to W age progression which was recently found in the Serbian Timok area (von Quadt et al., 2003a, b; see also Clark and Ullrich, 2004).

Structural and geodynamic setting

All Srednogorie-type plutonic rocks postdate weak regional metamorphism dated at 105–99 Ma (Velichkova et al., 2004) in southern sectors of the Panagyurishte region. The Central Srednogorie basin has a rhomb-shape, which is displaced along the Maritsa (or Iskar-Yavoritsa) strike-slip shear zone along the southern margin of the Panagyurishte region, with a dextral transtensional, N-side down displacement (Ivanov et al., 2002). The shear zone formed during intrusion of granites, which were dated between 84 and 78 Ma (Kamenov et al., 2002; von Quadt et al., 2003b). The northernmost Rhodopian metamorphic complex was uplifted and partly exhumed during this motion (Aiello et al., 1977; Ivanov et al., 2002; Krohe and Mposkos, 2002).

Evidence for ca. N–S extension also comes from orientations of both magmatic dykes and mineralized extensional veins: Interestingly, the quartz-monzonite dyke of Elatsite is E-trending and steeply N-dipping (Fanger, 2002; von Quadt et al., 2002). This suggests N–S extension during intrusion, at ca. 92 Ma. Sibson (2001), Robert and Poulsen (2001), Tosdal and Richards (2001) and Drew (2003) proposed models explaining formation of ore veins within a mesh where the maximum principal stress orientations are parallel to extensional ore veins. This is applied to the region and two examples are shown in Fig. 4. Mineralized (magnetite, molybdenite) quartz veins always formed during earliest stages of mineralization. Within several ore deposits, these trend E–W to ENE–WSW (e.g., Elatsite, Fanger, 2002; Medet). The ca. ENE–WSW trend of Elatsite also suggests NNW–SSE extension. The host intrusion is dated at ca. 92 Ma. In contrast, Assarel, Elshitsa, and some other ore deposits show a predominant N–S trend of ore-bearing quartz veins (Fig. 4 for Assarel) showing ca. E–W extension, although some E–W-trending, thinner mineralized quartz veins occur at Assarel, possibly recording the switch in extension directions.

The ca. 92 Ma old NNW–SSE extension is incompatible with a dextral shear along the WNW-trending Iskar-Yavoritsa shear zone according to classical structural models summarized in Harding (1974) and Mandl (1988). Dextral shear along the WNW-trending Iskar-Yavoritsa shear zone implies ca. N–S compression and ca. E–W exten-

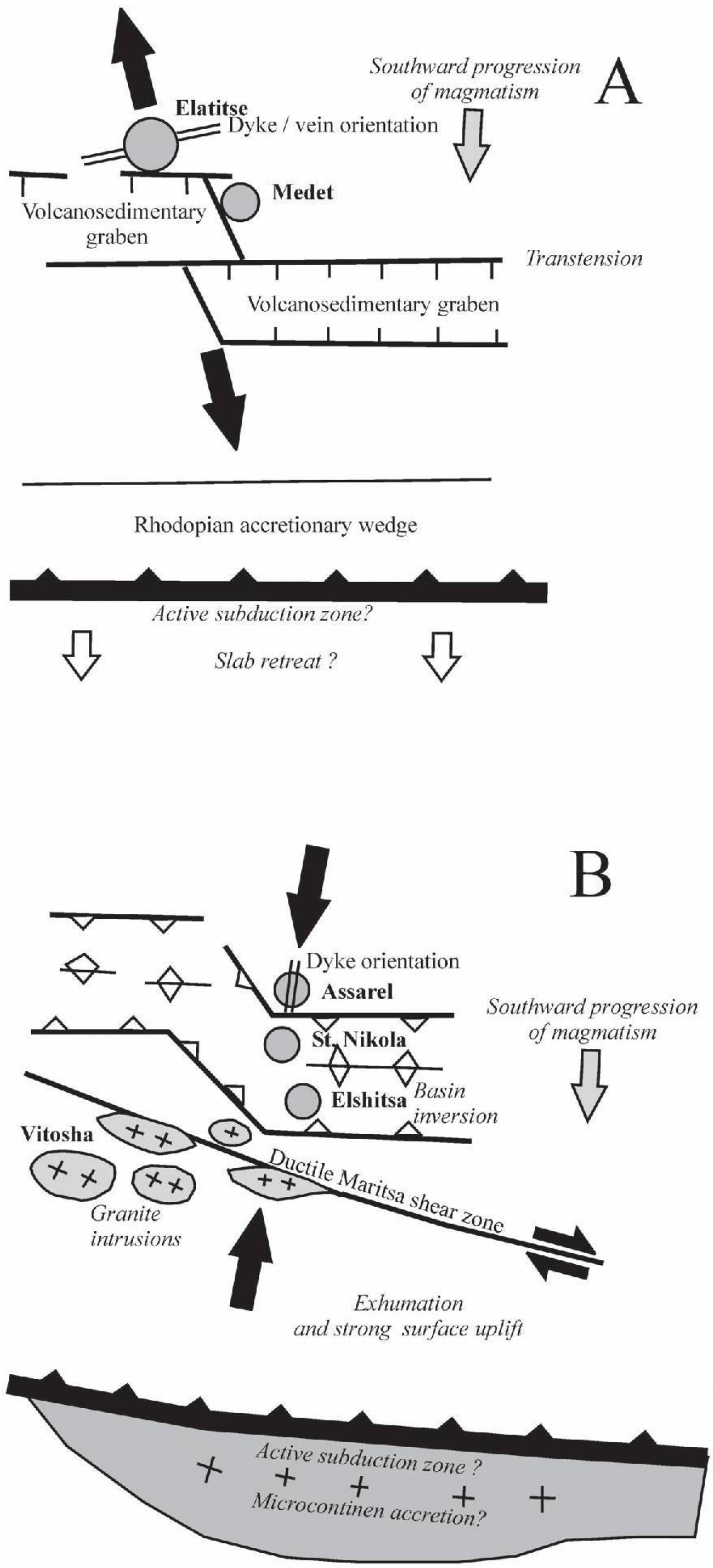

Fig. 5 Simplified geological models, adopting the subduction model for formation of the Banatite Belt, for the tectonic evolution of the Central Southern Srednogorie Zone and the change of structural setting.
A — Initial stage (92–91 Ma) with ca. NNW–SSE extension.
B — Second stage (86–78 Ma) with ca. N–S shortening. For discussion, see text.

sion as typically recorded in most of extensional veins at Assarel. This is perpendicular to the deformation during the 92 Ma-period. Consequently, the structural setting changed during this second period.

Therefore, structural data from magmatic dykes and mineralized veins show an interesting shift of extensional directions. The initial extension was N–S as the ca. 92 Ma old dyke at Elatsite indicates. The magmatic dykes and mineralized veins, dated at ca. 92–91 Ma, argue for NNW–SSE to N–S extension (Fig. 5A). The activation of the dextral Iskar-Yavoritsa wrench corridor between ca. 84 and 78 Ma suggests E–W extension. These relationships suggest a possible reversal of large scale dextral wrenching of the E-trending Srednogorie Zone from initial sinistral to late stage dextral displacement (Fig. 5B). The southernmost of these granitoids intruded at depths of 4–6 kbar (Georgiev and Lazarova, 2003; Ivanov et al., 2002) implying a significantly higher rate of exhumation since intrusion compared to shallow-level intrusions in northern sectors of the Panagyurishte region. As the northernmost granitoids and basement rocks are unmetamorphic (Alpine metamorphic temperatures <300 °C), these relationships suggest a northward, Late Cretaceous tilting and exhumation of southernmost granitoids and basement gneisses, which were overprinted by greenschist facies metamorphism (metamorphic temperatures >400 °C) at 105–99 Ma (Velichkova et al., 2004). Exhumation and tilting were likely contemporaneous with the intrusions of the in part ductilely deformed Cretaceous granitoids. Exhumation occurred within a transtensive/transpressive setting, as some of these granitoids were deformed during solidification within the WNW-trending dextral steep Iskar-Yavoritsa shear zone (Ivanov et al., 2002)

The causes of magmatism and formation of sedimentary basins are a matter of intense debate. Three alternative models have been proposed, (1) rift, (2) northward subduction of oceanic crust, and (3) post-collisional slab break-off (see Berza et al., 1998; Ciobanu et al., 2002, and Neubauer, 2002 for detailed discussions). In the subduction model, the southward shift of magmatism and extensional sedimentary basin formation would be possibly triggered by a southward retreat of the subduction zone (Fig. 5A). The subsequent change to N–S compression (during the 86–78 Ma period) could be explained by accretion of a microcontinent to the subduction complex, which exerted horizontal contractional forces perpendicular to the strike of the continental margin (Fig. 5B). A similar model of Late Cretaceous to Palaeogene stepwise accretion of microcontinental blocks was recently proposed for the Rhodopian metamorphic complex (Barr et al., 1999). Adopting the slab break-off model, the change in palaeostress orientations can be explained in a similar way. The initial stage of slab break-off would have resulted in a short period of extension perpendicular to strike of the orogen (e.g., Wortel and Spakman, 2000). Subsequent shortening may have been driven by final collision or large-scale plate motion. However, the present state of knowledge does not allow final distinction between the subduction and slab break-off model. The large uncertainty is the existence of major remnants of subductable oceanic lithosphere to the south of the Rhodopian accretionary complex during Late Cretaceous times (see Ricou et al., 1998; Neugebauer et al., 2001; Neubauer et al., 2003 for discussion).

Possible Tertiary thermal overprint

The low-energy release steps reported in the Ar-release spectra of samples 1b, 2, 4, and 5 are interpreted to likely record the age of a last thermal overprint during Eocene/Early Oligocene times. These patterns show indications of staircase patterns where the age of the first, youngest increment may be interpreted to record the minimum age of a very low- to low-grade thermal overprint. This can also include hydrothermal alteration, which is likely unrelated with mineralizing fluids.

The data indicate, therefore, some weak thermal overprint during the Eocene/Early Oligocene (at ca. 40–32 Ma) as indicated by ages reported in the low-temperature gas release steps of samples 1b, 2, 4, and 5. However, this interpretation needs further confirmation by Ar-dating of more altered samples, which have been excluded for this study. The reason for the partial resetting of the Ar-isotopic system at ca. 40 Ma may be the same as for the Eocene remagnetisation recorded by palaeomagnetism in the northerly adjacent Balkan Zone (Jordanova et al., 2001). This would imply that final N–S shortening during Eocene also affected the Srednogorie Zone. Furthermore, Eocene tectonic activity, mainly N–S shortening, is also recorded in the southern Rhodopian metamorphic core complex (e.g., Krohe and Mposkos, 2002; Kaiser-Rohrmeier et al., 2004).

Conclusions

The results allow to draw the following major conclusions:

(1) Together with recently reported U–Pb zircon ages (Table 1), the new $^{40}Ar/^{39}Ar$ ages show

the duration of intrusions of subvolcanic bodies and the volcanic surface expressions between ca. 92 and 78 Ma.

(2) The data confirm a principal north-to-south progression of magmatism, crossing the principal E–W trend of the Banatite Belt in this region. The N to S progression could represent trench-ward motion as some models assume a Late Cretaceous subduction/trench to the south of the Rhodopian massif.

(3) A change in the regional stress field occurred between the 92–90 Ma and 84–78 Ma periods. In the earlier stage, N–S extension prevailed whereas in the second stage ca. N–S shortening was predominant.

(4) There is evidence for a weak thermal overprint, which affected the northern sectors of the Srednogorie Zone. This is consistent with Eocene remagnetization recorded by palaeomagnetism in the northerly adjacent Balkan zone.

Acknowledgements

We gratefully acknowledge careful reviews by Robert Moritz and Thomas Pettke as well as suggestions of Thomas Driesner for the final version. We also acknowledge support by the "GEODE Grants for Visit Program" to SV. Work has been carried out within the project P15.646-GEO of the Austrian Research Foundation.

References

Aiello, E., Bartolini, C., Bocaletti, M., Gocev, P., Karagjuleva, J., Kostadinov, V. and Manetti, P. (1977): Sedimentary features of the Srednogorie Zone (Bulgaria), an Upper Cretaceous intra-arc basin. *Sed. Geol.* **19**, 39–68.

Arnaudov, V., Amov, B., Bratnitzkii, B. and Pavlova, M. (1989): Isotopic geochronology of magmatic and metamorphic rocks from Balkanides and Rhodope massif. XIV Congress of CBGA, Sofia, Sept. 1989, 1154–1157 (in Russian).

Barr, S.R., Temperley, S. and Tarney, J. (1999): Lateral growth of the continental crust through deep level subduction-accretion: arc-evaluation of central Greek Rhodope. *Lithos* **46**, 69–94.

Berza, T., Constantinescu, E. and Vlad, S.N. (1998): Upper Cretaceous magmatic series and associated mineralisation in the Carpathian-Balkan Orogen. *Resource Geol.* **48**, 291–306.

Bocaletti, M., Manetti, P. and Peccerillo, A. (1974): The Balkanids as an instance of back-arc thrust belt: Possible relation with the Hellenids. *Geol. Soc. Am. Bull.* **85**, 1077–1084.

Bocaletti, M., Manetti, P., Peccerillo, A. and Stanisheva-Vasilieva, G. (1978): The Late Cretaceous high-potassium volcanism in eastern Srednogorie, Bulgaria. *Geol. Soc. Am. Bull.* **89**, 439–447.

Burg, J.P., Ivanov, Z., Ricou, L.E., Dimor, D. and Klain, L. (1990): Implication of shear-sense criteria for the tectonic evolution of the Central Rhodope massif, southern Bulgaria. *Geology* **18**, 451–454.

Burg, J., Ricou, L., Ivanov, Z., Godfriaux, I., Dimov, D. and Klain, L. (1993): Crustal-scale thrust complex in the Rhodope massif. Structure and kinematics. *Bull. Geol. Soc. Greece* ***XXVIII***, 71–85.

Chambefort, I., von Quadt, A. and Moritz, R. (2003): Volcanic environment and geochronology of the Chelopech high-sulfidation epithermal deposit, Bulgaria: regional relationship with associated deposits. European Union of Geosciences 12th Biennial Meeting, Nice, France, 6–11 April 2003. Abstract on CD: EAE03-A-00569.

Channell, J.E.T. and Kozur, H. (1997): How many oceans? Meliata, Vardar, and Pindos oceans in Mesozoic Alpine paleogeography. *Geology* **25**, 183–186.

Ciobanu, C.L., Cook, N.G. and Stein, H. (2002): Regional setting and Re–Os age of ores at Ocna de Fier Dognecea (Romania) in the context of the banatitic magmatic and metallogenic belt. *Mineralium Deposita* **37**, 541–567.

Clark, A.H. and Ullrich, T.D. (2004): $^{40}Ar–^{39}Ar$ age data for andesitic magmatism and hydrothermal activity in the Timok Massif, eastern Serbia: implications for metallogenetic relationships in the Bor copper-gold subprovince. *Mineralium Deposita* **39**, 256–262.

Cotta, B. von (1864): Über Eruptivgesteine und Erzlagerstätten in Banat und Serbien. Edit. V. Braunmüller, Wien, 105 pp.

Dabovski, C. (1988): Precambrian in the Srednogorie Zone (Bulgaria). In: Cogné, J., Kozhoukharov, D. and Kräutner, H.G. (eds.): Precambrian in younger fold belts, Essex, p. 841–847.

Drew, L.J. (2003): Model of the copper and polymetallic vein family of deposits – applications in Slovakia, Hungary, and Romania. *Int. Geol. Rev.* **45**, 143–156.

Fanger, L. (2002): Geology of a porphyry copper (-Au-PGE) ore deposit: Elatsite, Bulgaria. In: Moritz, R. and von Quadt, A. (eds.): GEODE Workshop on the Srednogorie Zone. April 2002. Sofia, Bulgaria, Abstract volume, p. 3.

Foose, R.M. and Manheim, F. (1975): Geology of Bulgaria. *Am. Assoc. Petrol. Geol. Bull.* **59**, 303–335.

Georgiev, N. and Lazarova, A. (2003). Magma mixing in Upper Cretaceous plutonic bodies in the southwestern parts of the Central Sredna gora zone, Bulgaria. *C. R. Bulg. Acad. Sci.* **56**, 4, 47–52.

Harding, T.P. (1974): Petroleum traps associated with wrench faults. *Am. Assoc. Petrol. Geol. Bull.* **58**, 1290–1304.

Ivanov, Z., Georgiev, N. Lazarova, A. and Dimov, D. (2002): New model of Upper Cretaceous magma emplacement in the southwestern parts of Central Sredna Gora zone, Bulgaria. *Geologica Carpathica* **53**, spec issue, Proc. the XVII. Congress of CBGA, Bratislava (CD version).

Jankovic, S. (1997): The Carpatho-Balkanides and adjacent area: a sector of the Tethyan Eurasian metallogenic belt. *Mineralium Deposita* **32**, 426–433.

Jordanova, N., Henry, B., Jordanova, D., Ivanov, Z., Dimov, D. and Bergerat, F. (2001): Paleomagnetism in northwestern Bulgaria: geological implications of widespread remagnetization. *Tectonophysics* **343**, 79–92.

Kamenov, B., von Quadt, A. and Peytcheva, I. (2002): New insight into petrology, geochemistry and dating of the Vejen pluton, Bulgaria. *Geochem. Miner. Petrol.* **39**, 3–25.

Kaiser-Rohrmeier, M., Handler, R., von Quadt, A. and Heinrich, C. (2004): Hydrothermal Pb–Zn ore formation in the Central Rhodopian Dome, south Bulgaria: Review and new time constraints from Ar–Ar geochronology. *Schweiz. Mineral. Petrogr. Mitt.* **84**, 37–58.

Karagjuleva, J., Kostadinov, V., Tzankov, Tz. and Gocev, P. (1974): Structure of the Panagjuriste strip east of the Topolnitsa river. *Bull. Geol. Inst., ser. Geotectonics* **13**, 231–301.

Kehayov, R., Bogdanov, K., Fanger, L., von Quadt, A., Pettke, T. and Heinrich, C. (2003): The fluid chemical evolution of the Elatsite porphyry Cu-Au-PGE deposit, Bulgaria. In: Elioupoulos, D.G. et al. (eds.): Mineral exploration and sustainable development. Proceedings 7th Biennial SGA Meeting, Athens, Greece, 24–28 August, 2003, Millpress, Rotterdam, p. 1173–1176.

Kouzmanov, K., Ramboz, C., Lerouge, C., Deloule, E., Beaufort, D. and Bogdanov, K. (2003): Stable isotope constraints on the origin of epithermal Cu–Au and related porphyry copper mineralisations in the southern Panagyurishte district, Srednogorie Zone, Bulgaria. In: Elioupoulos, D.G. et al. (eds.): Mineral exploration and sustainable development. Proceedings 7th Biennial SGA Meeting, Athens, Greece, 24–28 August, 2003, Millpress, Rotterdam, p. 1181–1184.

Krohe, A. and Mposkos, E. (2002): Multiple generations of extensional detachments in the Rhodope Mountains (northern Greece): evidence of episodic exhumation of high-pressure rocks. In: Blundell, D.J., Neubauer, F. and von Quadt, A. (eds.): The timing and location of major ore deposits in an evolving orogen. *Geol. Soc. (London) Spec. Publ.* **204**, 151–178.

Ludwig, K.R. (2001): Isoplot/Ex – A Geochronological Toolkit for Microsoft Excel. *Berkeley Geochronological Center Special Publication* **No. 1a**.

Mandl, G. (1988): Mechanics of tectonic faulting: models and basic concepts. Elsevier, Amsterdam, pp. XIV + 407.

McDougall, I. and Harrison, M.T. (1999): Geochronology and Thermochronology by the $^{40}Ar/^{39}Ar$ Method. 2nd ed, Oxford University Press, Oxford, 299 pp.

Neubauer, F. (2002): Contrasting Late Cretaceous to Neogene ore provinces in the Alpine-Balkan-Carpathian-Dinaride collision belt. In: Blundell, D.J., Neubauer, F. and von Quadt, A. (eds.): The timing and location of major ore deposits in an evolving orogen. *Geol. Soc. (London) Spec.Publ.* **204**, 81–102.

Neubauer, F., Dallmeyer, R.D., Dunkl, I. and Schirnik, D. (1995): Late Cretaceous exhumation of the metamorphic Gleinalm dome, Eastern Alps: kinematics, cooling history and sedimentary response in a sinistral wrench corridor. *Tectonophysics* **242**, 79–89.

Neubauer, F., Heinrich, C. and GEODE Working Group incl. Tomek, C., Lips, A., Nakov, R., von Quadt, A., Peytcheva, I., Handler, R. Bonev, I., Ivascanu, P., Rosu, E., Ivanov, Z., Kaiser-Rohrmeier, M. and others (2003): Late Cretaceous and Tertiary geodynamics and ore deposit evolution of the Alpine-Balkan-Carpathian-Dinaride orogen. In: Eliopoulos, D. et al. (eds.): Mineral Exploration and sustainable development. Millpress, Rotterdam, p. 1133–1136.

Neugebauer, J., Greiner, B. and Appel, E. (2001): Kinematics of Alpine–West Carphian orogen and palaeogeographic implications. *J. Geol. Soc. (London)* **158**, 97–110.

Okay, A.I., Satir, M., Tüysüz, O., Akyüz, S. and Chen, F. (2001): The tectonics of the Strandja Massif: late Variscan and mid-Mesozoic deformation and metamorphism in the northern Aegean. *Int. J. Earth Sci.* **90**, 217–233.

Peytcheva, I. and von Quadt, A. (2003): U–Pb-zircon isotope system in mingled and mixed magmas: an example from Central Srednogorie, Bulgaria. *Geophys. Res. Abstracts* **5**, 09177, Nice, (electronic version).

Peytcheva, I., von Quadt, A., Kamenov, B., Ivanov. Z.H. and Geogiev, N. (2001): New isotope data for Upper Cretaceous magma emplacement in the Southern und South-Western parts of Central Srednogorie. *Rom. J. Mineral Deposits* **79** suppl. 2, 82–83.

Peytcheva, I., von Quadt, A., Kouzmanov, K. and Bogdanov, K. (2003): Elshitsa and Vlaykov Vruh epithermal and porphyry Cu (-Au) deposits of Central Srednogorie, Bulgaria: source and timing of magmatism and mineralization. In: Eliopoulos et al. (eds.): Mineral exploration and sustainable development. Millpress Rotterdam, p. 371–373.

Popov, P.N. (1987): Tectonics of the Banat-Srednogorie Rift. *Tectonophysics* **143**, 209–216.

Popov, P. (1996): On the tectono-metallogenic evolution of the Balkan peninsula Alpides. *UNESCO – IGCP project No 356* 1, 5–17.

Popov, P. and Popov, K. (2000): General geologic and metallogenic features of the Panagyrishte ore region. In: Strashimirov, S. and Popov, P. (eds.): Geology and metallogeny of the Panagyurishte ore region (Srednogorie Zone, Bulgaria). Guide to Excursions A and C. ABCD-GEODE 2000 Workshop, Borovets Bulgaria, p. 1–7.

Quadt, A. von, Peytcheva, I., Kamenov, B., Fanger, L. and Heinrich, C.A. (2002): The Elatsite porphyry copper deposit of the Panagyurishte ore district, Srednogorie Zone, Bulgaria: U–Pb zircon geochronology and isotope-geochemical investigations of ore genesis. In: Blundell, D., Neubauer, F. and Quadt, A. von (eds.): The timing and location of major ore deposits in an evolving orogen. *Geol. Soc. Spec. Publ.* **204**, 119–135.

Quadt, A. von, Peytcheva, I., Heinrich, C., Frank, M., Cvetkovic, V. and Banjesevic, M. (2003a): Evolution of the Cretaceous magmatism in the Apuseni-Timok-Srednogorie metallogenic belt and implications for the geodynamic reconstructions: new insight from geochronology, geochemistry and isotope studies. In: Neubauer, F. and Handler, R. (eds.): Programme and Abstracts, Fibal ABCD-GEODE 2003 Workshop, Seggauberg, Austria, 22–24 March 2003, p. 60.

Quadt, A. von, Peytcheva, I. and Cvetkovic, V. (2003b): Geochronology, geochemistry and isotope tracing of the Cretaceous magmatism of East-Serbia and Panagyurishte district (Bulgaria) as part of the Apuseni-Timok-Srednogorie metallogenic belt in Eastern Europe. In: Eliopoulos et al. (eds.): Mineral exploration and sustainable development. Millpress Rotterdam, p. 407–410.

Ricou, L.E., Burg, J.P., Godfriaux, I. and Ivanov, Z. (1998): Rhodope and Vardar: the metamorphic and the olistostromic paired belts related to the Cretaceous subduction under Europe. *Geodinamica Acta* **11**, 285–309.

Robert, F. and Poulsen, K.H. (2001): Vein formation and deformation in Greenstone gold deposits. In: Richards, J.P. and Tosdal, R.M. (eds.): Structural controls on ore genesis. *Rev. Econ. Geol.* **14**, 111–155.

Sibson, R.H. (2001): Seismogenic framework for hydrothermal transport and ore deposition. *Econ. Geol. Rev*. **14**, 25–50.

Steiger, R.H. and Jäger, E. (1977): Subcommission on geochronology: Convention on the use of decay constants in geo- and cosmochronology. *Earth Planet. Sci. Lett.* **36**, 359–362

Stoykov, S., Peytcheva, I., von Quadt, A., Moritz, R., Frank, M. and Fontignie, D. (2004): Timing and magma evolution of the Chelopech volcanic complex (Bulgaria). *Schweiz. Mineral. Petrogr. Mitt.* **84**, 101–117.

Strashimirov, S. and Popov, P. (2000): Geology and metallogeny of the Panagyurishte ore region (Srednogorie Zone, Bulgaria). ABCD-GEODE 2000 Work-

shop, Borovets, Guide to Excursions (A and C), Sofia, pp. 52.
Strashimirov, S., Petrunov, R. and Kanzirski, M. (2002): Porphyry-copper mineralization in the central Srednogorie Zone, Bulgaria. *Mineralium Deposita* **37**, 587–598.
Tarkian, M., Hüken, U., Tokmakchieva, M. and Bogdanov, K. (2003): Precious-metal distribution and fluid inclusion petrography of the Elatsite porphyry copper deposit, Bulgaria. *Mineralium Deposita* **38**, 261–181.
Tosdal, R.M. and Richards, J.P. (2001): Magmatic and structural controls on ore genesis. *Rev. Econ. Geol.* **14**, 157–181.
Velichkova, S., Handler, R. and Neubauer, F. (2001): Preliminary $^{40}Ar/^{39}Ar$ mineral ages from the Central Srednogorie Zone, Bulgaria: Implications for Cretaceous geodynamics. *Rom. J. Mineral Deposits* **79**, 112–113.
Velichkova, S.H., Handler, R., Neubauer, F. and Ivanov, Z. (2004): Variscan to Alpine tectonothermal evolution of the Central Srednogorie unit, Bulgaria: constraints from $^{40}Ar/^{39}Ar$ analysis. *Schweiz. Mineral. Petrogr. Mitt.* **84**, 133–151.
Wijbrans, J.R., Pringle, M.S., Koopers, A.A.P. and Schveers, R. (1995): Argon geochronology of small samples using the Vulkaan argon laserprobe. *Proc. Kon. Ned. Akad. Wetensch.* **98**(2), 185–218.
Willingshofer, E., Neubauer, F. and Cloetingh, S. (1999): Significance of Gosau basins for the upper Cretaceous geodynamic history of the Alpine-Carpathian belt. *Phys. Chemistry Earth Part A: Solid Earth Geodesy* **24**, 687–695.
Wortel, M.J.R. and Spakman, W. (2000): Subduction and slab detachment in the Mediterranean-Carpathian region. *Science*, **290**, 1910–1017.

Received 19 October 2003
Accepted in revised form 23 July 2004
Editorial handling: T. Driesner

Appendix

Description of samples

Sample 1: Porphyric quartz monzonite with a fine-grained groundmass (average grain sizes ca. 0.03–0.05 mm) of quartz, feldspar, and plagioclase, and amphibole phenocrysts of 1–3 mm in size. Some patchy alteration with finest-grained sericite occurs mainly within plagioclase. Plagioclase displays a pronounced optical zoning. Greenish amphibole is internally homogeneous, poor in inclusions except ore-rich rims and shows only in a few cases some secondary alteration. Biotite occurs in aggregates replacing amphibole. Further minerals are quartz, sphene, epidote, apatite and secondary calcite.

Sample 2: Decimeter-sized blocks of porphyric, brecciated andesite occur within a fine-grained andesitic matrix. Blocks were used for dating and comprise coarse, equidimensional grains (average grain size 2–3 mm), of optically zoned plagioclase, unzoned amphibole and subordinate brown biotite as the main constituents within a finer-grained matrix with similar minerals, which also include biotite. Alteration is weak and mainly affected plagioclase and very subordinately biotite.

Sample 3: Porphyric granodiorite with a fine-grained groundmass (average grain size is ca. 0.05 mm) and ca. 1–3 mm large phenocrysts of K-feldspar, plagioclase, quartz and amphibole. Greenish amphibole is rich in inclusions like biotite, plagioclase, opaque minerals, sphene, apatite and rare chlorite along rims. Plagioclase phenocrysts show a pronounced oscillatory zoning. Further minerals are sphene, opaque minerals and apatite.

Sample 4: The granodiorite consists mainly of skeletal quartz graphically intergrown with plagioclase and subordinate K-feldspar. Amphibole is rare and occurs in millimeter-sized subhedral grains. Some amphibole grains are replaced by chlorite along margins. Plagioclase contains much very fine-grained sericite. Biotite is occasionally replaced by chlorite, leucoxene and epidote.

Sample 5: Porphyric andesite with phenocrysts of green amphibole, plagioclase and clinopyroxene. Amphiboles are ca. 0.2–0.7 mm in size, optically homogeneous and contain only a few inclusions with predominant opaque minerals and apatite and few quartz and plagioclase grains. Secondary alteration occurs along grain boundaries of mainly plagioclase. Secondary minerals comprises sericite, greenish biotite and chlorite of ca. 0.03 to 0.04 mm size.